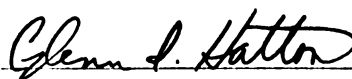This is to certify that the

thesis entitled

**LACTATION-ASSOCIATED REDISTRIBUTION OF THE
GLIAL FIBRILLARY ACIDIC PROTEIN WITHIN THE SUPRAOPTIC
NUCLEUS OF THE RAT: AN IMMUNOCYTOCHEMICAL STUDY**

presented by

Adrienne Kay Salm

has been accepted towards fulfillment
of the requirements for

_____M.A._____degree in Psychology_

Glenn I. Hatton

Major professor

Date *8 Sept 1983*

O-7639

LACTATION-ASSOCIATED REDISTRIBUTION OF THE GLIAL

FIBRILLARY ACIDIC PROTEIN WITHIN THE SUPRAOPTIC NUCLEUS

OF THE RAT:AN IMMUNOCYTOCHEMICAL STUDY

By

Adrienne Kay Salm

A THESIS

Submitted to

Michigan State University

in partial fulfillment of the requirements

for the degree of

MASTER OF ARTS

Department of Psychology

1983

ABSTRACT

LACTATION-ASSOCIATED REDISTRIBUTION OF THE GLIAL FIBRILLARY ACIDIC PROTEIN WITHIN THE SUPRAOPTIC NUCLEUS OF THE RAT: AN IMMUNOCYTOCHEMICAL STUDY

By

Adrienne Kay Salm

Previous electron microscopical evidence has demonstrated a lactation or dehydration-induced disappearance of glial processes normally interposed between magnocellular neuroendocrine cell (MNC) somata. These data suggested the hypothesis that glia actively retract their processes when MNCs are highly active. This hypothesis was investigated at the light microscopic level in the supraoptic nuclei (SON) of lactating and estrous rats. The distribution of components of the glial cytoskeleton was visualized using antibodies against the glial fibrillary acidic protein (GFAP). The lateral hypothalamic area (LHA) was also sampled. Computerized image analysis was employed to assess changes in the distribution of this protein concomitant with lactation. Statistical analysis revealed a redistribution of GFAP in the SON of lactating, as compared to estrous, animals which reflected a reduction in the number of glial processes. No such changes were found in the LHA. These results demonstrate a morphological lability of astrocytes in response to a physiological stimulus.

This is dedicated to the late

Dr. David Karl Bliss,

who first encouraged me to do research.

Acknowledgments

Many thanks, first, to Dr. Glenn I. Hatton for his support, guidance, encouragement and faith, during the development of this thesis. Also, recognition and thanks are due to Mr. Kenneth Smithson for general technical assistance throughtout the project. In addition, his astute analysis of the problems inherent in computerized image analysis, and his ability to surmount them by creating excellent software, made the use of such technology possible for this thesis. Acknowledgment is also due Dr. Gajanan Nilaver for the generous gift of his anti-GFAP serum. I am grateful also to Dr. Richard Dubes for the use of the facilities at the Pattern Recognition and Image Analysis Laboratory at MSU. Dr. William Bukowski deserves a special thanks for contributing his time and expertise in executing the BMDP statistical program used for analysing much of the data. I'm also grateful to Dr. John Gill for illuminating the utility of split-plot designs in biological research. I'd like to thank my other committee members, Dr. Antonio Nunez, Dr. Charles Tweedle, and Dr. Charles Wilson for comments, critiques, and moral support. Also, Dr. Peter Cobbett has been immeasurably helpful with editorial and scientific comments on an earlier draft of the manuscript. Janice Harper, Betty Simon, and Carla Tiller have my undying gratitude for

their expert secretarial assistance. Finally, to my
family, particularly my parents, and friends, thank-you
for having faith and supporting me in all of my efforts.
This research was supported by NIH grant # 09140.

TABLE OF CONTENTS

LIST OF TABLES

LIST OF TABLES-cont.

LIST OF FIGURES

LIST OF ABBREVIATIONS

3V	THIRD VENTRICLE
BV	BLOOD VESSEL
GFAP	GLIAL FIBRILLARY ACIDIC PROTEIN
LHA	LATERAL HYPOTHALAMIC AREA
NC	NUCLEUS CIRCULARIS
OT	OPTIC TRACT
PG	PIAL-GLIAL PLEXUS
SCN	SUPRACHIASMATIC NUCLEUS
SON	SUPRAOPTIC NUCLEUS

INTRODUCTION

In recent years the list of functions attributed to
neuroglia has grown to include much more than merely being,
as Virchow (1840) named them, the "glue" of the nervous
system. It has been repeatedly demonstrated both in vitro
and in vivo that astrocytes are capable of modifying and
responding to their enviroments (see Varon and Somjen, 1979,
for review). Ultrastructural, morphological, and biochemical
changes have been variously observed in astrocytes to be
associated with mechanically produced CNS injuries (Bignami
and Dahl, 1973; Latov et al.,1979); irradiation (Maxwell and
Kruger,1965); topical alumina (Harris, 1973); nerve
sectioning (Vaughn and Pease,1970); hypertension (Hanakita
et al.,1980); and hypoxia (Landis and Reese, 1981). Laursen
and Diemer (1980) have shown that ultrastructural changes
also occur in astrocytes during increased CNS ammonium
levels created by portocaval anastomosis.

At the light microscopic level, astrocytic plasticity
has been demonstrated in response to pharmacological
manipulations. Morphological changes have been induced in
immature astrocytes in primary monolayer cultures by the
addition into the medium of dibutryl cyclic adenosine
monophosphate (Kimelberg et al., 1980; Manthorpe et al.,
1979; Moonen et al, 1976); norepinephrine (Narumi et al.,

1

1978; Steig et al., 1980) and prostaglandins (Tardy et al., 1981). Such changes are positively correlated with the polymerization into filaments of the glial fibrillary acidic protein (GFAP) which exists in these cells. GFAP is a 10 nm intermediate filament protein with a molecular weight of 49-55 daltons which is a major component of the mature astrocytic cytoskeleton (Liem, 1982).

This protein has received much attention in recent years because it serves as a "marker" of cells which are astroglial in origin (Bignami et al., 1980) and because its production and/or subsequent aggregation into filaments is often concomitant with other astrocytic changes associated with neuropathologies. In this regard, GFAP has become relevant to clinicians because its presence is associated with cerebral carcinomas (Duffy et al., 1978;1979; DeArmond et al., 1980 for review) fetal abnormalities (Pertti et al. 1980), and Alzheimer-type senile dementia, where both an increase in the amount of immunostainable GFAP (Duffy et al.,1980) and in the number of GFAP immunopositive astrocytes in cerebral cortex (Schechter et al., 1981) have been described.

Possible role of glia in neurosecretion.

Despite the growing evidence that neuroglia and GFAP are able to respond to a variety of stimuli, the current literature is, with a few exceptions, notably lacking in examples of glial lability in situ when conditions are both physiological and non-pathological. These exceptions include a number of descriptions which indicate that glial cells

within the hypothalamo-neurohypophysial neurosecretory system of the rat undergo biochemical changes which appear concurrently with the release of neurohypophysial hormones. Watson (1971) found that perfusion of the cerebral ventricles with a solution containing a high concentration of either potassium or phosphate, or the calcium chelator, EDTA, caused a marked and reversible increase in dry mass of hypothalamic paraventricular nucleus (PVN) astrocytes and nearby ependyma. He suggested that this was due to increased RNA and protein synthesis in these cells. In a similar study using interference microscopy and ultra-violet absorbtion microspectrography, Watson (1972) found that the dry mass of supraoptic nucleus (SON) and PVN astrocytes transiently increased with lactation or one day of dehydration.

In the SON and neural lobe, 14 days of substituting a 1.75% NaCl solution for drinking water, resulted in dramatic increase in the number of astrocytes labelled by injections of 3-H-thymidine (Paterson and LeBlond, 1977). These authors reported, however that the over-all number of astrocytes/ 100 neurons remained constant suggesting that some cell death occurred. Further evidence, although indirect, for a role of astrocytes in neurosecretion came from LaFarga et al. (1975) who were perhaps the first investigators to specifically describe the lack of a glial barrier between dehydration activated magnocellular neurons. Using electron microscopy (EM), these investigators also described unusually long membrane appositions between neurosecretory somata and further suggested that junctions similar to gap

junctions might exist between these as a basis for synchronous electrical activity.

More recently, at the EM level, Tweedle and Hatton (1976) also found that the conditon of dehydration was accompanied by a disappearance of glial elements which are normally interposed between the somata of neurons in the nucleus circularis (NC) and the SON. An active retraction of glial processes was hypothesized to account for the significant increases in soma-somatic apposition as these changes occur prior to the increased cell volume observed after brief dehydration (Hatton and Walters,1973; Hatton,1976). The reappearance of glial processes between neurosecretory somata with subsequent rehydration, provides further support for the participation of astrocytes in osmoregulation (Tweedle and Hatton, 1977).

The supposed retraction of fine glial processes has also been shown to occur within the SON and NC in lactating rats (Hatton and Tweedle, 1980; 1982). When compared to virgin females, Hatton and Tweedle found that the percentage of cells showing cell-cell contacts increased twelve-fold, from 3.5% to 44%. The increase in total membrane apposition was an even more dramatic 41-fold over that of the virgin females. A similar pattern of change was observed in NC, however to a lesser extent. Theodosis et al.(1981) also reported an apparent glial retraction from between the SON somata in lactating animals. Using a somewhat different sampling method, they calculated a five-fold increase in total surface membrane contact between SON cells of

lactating rats. The data from these latter two investigations indicate that lactation is a more effective stimulus than dehydration in promoting the disappearance of glial processes from between magnocellular neurons. In fact, the additional hormonal demand of one day of dehydration actually reduced the magnitude of this phenomena (Theodosis et al., 1981).

Elsewhere in this neurosecretory system, in the neurohypophysis (Tweedle and Hatton, 1980 a & b;1982) and in the PVN (Gregory, Tweedle and Hatton, 1980) glial retraction has likewise been described in association with the lactation and dehydration stimuli.

Statement of problem.

Thus far the evidence for changes in glial morphology has been indirect i.e., the absence of glial processes where they are normally observed. However, detecting changes in glial morphology is difficult at the high magnifications used in EM. Preliminary light level investigations using peroxidase anti-peroxidase (PAP) immunocytochemistry (ICC) for GFAP have shown an intricate glial reticulum within the SON (Salm and Hatton,1980) and NC in normally hydrated animals. The dense packing of neurons in these nuclei permits the suggestion that a change of the glial elements, be it a shortening of the processes or an aggregation of cytoplasmic GFAP into filaments could conceivably result in an increased neurosecretory cell apposition. In addition, astrocytes of both nuclei are invariably associated with vasculature and those of the SON occupy a particularly close

proximity to the arachnoid space, although whether any contact with CSF occurs is not known. Therefore, the glia of these nuclei appear to be positioned so as to be sensitive to osmotic or other cues in the blood and/or CSF, and to perhaps influence neurosecretory responses via changes in their own morphology. It may be possible to directly demonstrate that morphological changes of astrocytes have a role in the day to day running of the nervous system by documenting changes in these cells themselves. To this end, a method was developed to determine and compare the pattern and distribution of their cytoskelatal protein, GFAP, as visualized by PAP ICC with primary antibodies directed against GFAP. This was done in virgin estrous, and lactating rats.

METHODS

Subjects.

Subjects were twelve female Holtzman rats, 94- 98 days of age, divided into two groups of six: virgins in the estrous phase of their reproductive cycle (hereafter referred to as controls), and lactating animals 8 or 10 days post partum. All of the nursing animals had full litters, each nipple potentially being occupied during suckling. Animals were housed in a 12:12 light cycle with lab chow and water available ad libitum.

Procedure.

Rats were killed within four hours after the onset of the dark phase of the light cycle, a time when most of (prolactin excepted) estrous cycling hormones in estrous

animals are relatively low (Nequin,1979).

Time of estrus was determined by vaginal lavage yielding cornified epithelium. Animals were followed through at least two cycles and those having consistently equivocal smears were not used. It appeared important to control for the phase of the estrous cycle as there is a growing body of evidence which indicates estrogens may act to modify neurosecretory activity. Skowsky, Swan and Smith (1979) have reported an estrogen replacement stimulated rise in serum vasopressin in ovariectomized rats. Combined autoradiography and ICC indicate that estrogen receptors are localized to hormone containing cells of magnocellular nuclei (Sar and Stumpf, 1980; 1981; Rhodes, Morrell and Pfaff, 1981). Behavioral data indicate that volemic thirst appears to be influenced by the estrous cycle, being least apparent during estrus (Findlay, Fitzsimmons, and Kucharczyk, 1979). Negoro et al. (1973) and Freund-Mercier and Richard (1977) have found that PVN neurons that project to the posterior pituitary vary in their spontaneous and stimulation induced firing rates over the course of the estrous cycle. By monitoring neurosecretory activity during normal reproductive cycles in ovariectomized animals with and without estrogen replacement and during pregnancy and lactation, Swaab and Jongkind (1970) found that the greatest level of activity coincided with (reported) high levels of plasma gonadotrophs. However, no clear picture has yet emerged as to the exact relation between the gonadotrophins and neurohypophysial secretory activity.

Histology.

Following transcardiac perfusion with 1%
glutaraldehyde, 2.5% paraformaldehyde in 0.1M cacodylate
buffer (pH 7.25), brains were dissected from the skull,
trimmed into hypothalmic blocks, immersed in fixative until
block was firm, and rinsed extensively in Tris buffered
saline (see Appendix A) for 48 hours. At this time, a
randomly selected code number was assigned to each brain by
an associate, in order that subsequent operations be
performed without knowledge of the experimental group
membership. The block was dehydrated in ethanol and embedded
in polyethylene glycol for 15um sectioning with a rotary
microtome, according to the procedure of Smithson et
al.(1983). Sections were cut in either coronal or horizontal
planes with three brains per orientation per group. Every
third section from the coronal group, and all sections from
the horizontal group were collected and rehydrated for
immunocytochemical processing with a primary antiserum
raised against GFAP. Additional sections were processed from
the coronally cut brains through areas identified as
containing NC.

Immunocytochemistry

For immunocytochemical processing, sections were
rehydrated in individual wells of a Plexiglas template which
requires 100ul of a given solution to adequately cover the
tissue. In order to eliminate non-specific staining and
allow for clearer visualization of stained processes a
pretreatment (Schachner et al.,1977) was first applied to

each section. Subsequently, the peroxidase-antiperoxidase immunostaining procedure of Sternberger (1974) was employed using primary antibodies against GFAP purified from human cerebral white matter (Latov et al., 1979).

In order to control for the inevitable variability which occurs between "batches" of immunocytochemically stained tissue, control and experimental sections were reacted simultaneously, with the exception of sections from one control and experimental brain each. In addition, the timing of each step of the protocol was held constant across "batches" of tissue. It was thus attempted to minimize method-induced variabilty. Details of the pretreament and ICC protocols are given in Appendix A.

After ICC was completed, sections were mounted, air dried, dehydrated in alcohol and couterstained with a 0.5% thionine solution. Following coverslipping with #1.5 coverslips the slides were examined under low magnification with a Zeiss microscope. For analysis of the SON of coronally sectioned brains 10 sections from the anterior and posterior SON each were selected. The boundary between these regions was semi-arbitrarily determined to be between the caudal part of suprachiasmatic nucleus and the most rostal portion of the medial paraventricular subnucleus. Equivocal sections were excluded from analysis. Also, based upon the overall intensity of the thionine stain, sections which were obviously thicker or thinner were omitted from these groups. For analysis of sections in the horizontal plane the five most dorsal and five most ventral sections were chosen.

Antiserum production and specificity

Antiserum against GFAP and preimmune serum were generous gifts of Drs. Gajanan Nilaver and Earl Zimmerman who prepared the antiserum according to the protocol of Dahl and Bignami (1975). Their procedures are summarized in Appendix A.

Preliminary data collection.

Preliminary data collection was performed on the NC of two experimental and two control animals. This was done in order to assess the sensitivity of the data collection methodolgy to presumptive changes in the distribution of astrocytic elements between control and experimental animals. NC was chosen for this analysis because of its apparent orderly neuronal arrangement and uncomplicated distribution of glial processes (Figure 1).

Methods.

All slides containing sections with NC were given individual code numbers by a colleague in order that all measurements be made without knowledge of experimental group. A microscope eyepiece reticule was used in making the following counts at 312.5X magnification:

1.The number of GFAP-positive glial processes appearing to be interposed directly between magnocellular somata.

2. The number of GFAP-positive glial processes visible which are not interposed between somata.

These measurments were done in order to ascertain

Figure 1. Photomicrograph of a 15 um section through the nucleus circularis. The section has been immunocytochemically stained using antibodies against GFAP. Large arrows point to glial processes. Small arrows points to neuronal cell bodies counterstained with thionine.

40 um
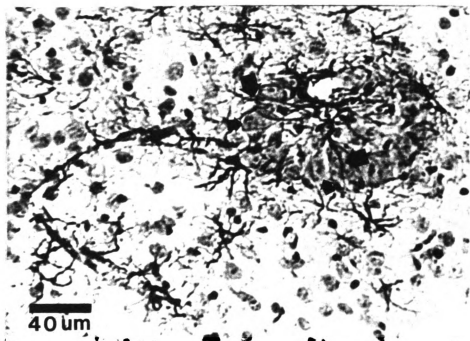
Figure 1.

whether the number of visible processes within the nucleus changed with experimental manipulation, and to determine where such changes might be localized in relation to the neurons therein.

To quantify these variables, the nucleus was centered within the field covered by the reticule as observed through the eyepiece. The incidence of each variable was counted for each grid square overlying the nucleus or a portion of it.

All numerical data were then converted to a value normalized for area, expressed as /cubic um, assuming sections to be ramdomly variable around a mean 15um thickness.

Analysis.

Preliminary testing of the data caused the hypothesis of equal variance to be rejected but one of equal coefficient of variation to be accepted. Accordingly, (Gill, 1978), the raw data were first transformed to logs prior to performing a standard t-test. This test was applied to detect differences between groups in the number of glial processes interposed between neuronal somata and in the total number of glial processes observed within the nucleus. Examination of the means for these two measures show that the means were virtually identical.

Table 1. Preliminary nucleus circularis data

	Mean processes not interposed /um^3 NC	Mean processes between somata /um^3 NC
CONTROL	-3.62 $\pm$ .63	-4.03 $\pm$ .22
LACTATING	-3.76 $\pm$ .30	-3.98 $\pm$ .41

Subsequent t-tests on these two measures confirmed that there were no significant differences between control and lactating animals.

Since changes in the amount of neurosecretory cell apposition had been shown to occur, both during dehydration and lactation (Tweedle and Hatton, 1977; Hatton and Tweedle, 1982), it was surprising that this was not reflected by changes in the number of observable processes in this nucleus. This finding prompted an evaluation of the methodology employed. Possible sources of the method's failure to detect differences were considered to be the following: (a) no changes actually occur under these conditions, and (b) the actual number of astrocytic processes don't change, but their dimensions do.

Possibility (a) was rejected on the basis of accumulated evidence cited in the initial pages of this thesis. Possibility (b) seemed the more reasonable in light of several considerations. First it was obvious that glial processes, as visualzed by PAP ICC for GFAP, vary in thickness (Figure 1). Simply counting the presence or absence of such processes ignores changes which may be

occurring in the dimensions of such processes. In addition, it is likely that GFAP ICC does not darkly stain the entire astrocyte. Intracellular injections of horseradish peroxidase (Picker and Goldring,1982) and metallic stains (personal observation) reveal quite a different picture of these cells. These techniques invariably reveal extensive velate material between the main processes. Such velate material is not invisible in immunostained astrocytes, but is seen as gradations of a light brown "wash" which is difficult to differentiate from any background staining and is still more difficult to quantify. It was for these reasons that a more sensitive method was sought. Such a method would have to exceed the capabilties of the previously employed methodology in these respects: improved resolution, i.e., able to discriminate minute differences in process width; improved ability to discriminate fine gradations in immunostaining densities and an ability to objectively and consistently quantify these differences. Such precision is found in computerized image analysis systems. One such system, the Eyecom II, is available at Michigan State University and was therefore used for this project. The images were produced by photographing each section through a microscope using a black and white negative film. The negatives were then scanned by the Eyecom II for image analysis.

Producing the image

    Optics. Before beginning photography, every precaution must be taken to optimize resolution with the available

equipment. Details concerning equipment and procedures are in Appendix A.

Photography. The major considerations here were the choices of film and developer, with special reference to the range of contrasts or densities which the film is capable of rendering with a certain developer. Since the Eyecom II system has a dynamic range of 2.2 density units, a fine grain (high resolution) film which could be developed to a similar density range was sought. Kodak Technical Pan 2415 35 mm negative film was chosen due to its high resolution (320 lines/mm) and compatible density range of 1.75 density units when developed with Kodak HC-110, dilution D. Also, this panchromatic film has the attractive feature of extended red sensitivity which makes it especially suited for depicting the reddish brown reaction product of DAB. To further enhance contrast, a #80 blue filter was used.

Another important factor related to the actual photography was holding constant the illumination of the specimen. This task required that not only the amount of light entering the system be the same, but also that it pass through each section in the same way, i.e., the field diaphragm and the substage condenser be similarly adjusted.

Illumination was held constant by metering the light transmitted through the Permount adjacent to each section using a Nikon light meter. The light sensor was held to a Nikon focusing eyepiece connected in series to the mechanical tube and camera. The voltage of the light source was then adjusted to give a 6uA $\pm$ .5 uA reading on the light

meter. Prior to photography, the substage aperature was adjusted to 80% of its maximum as recommended for modified Köhler illumination. This position was marked and checked throughout the photography process.

Random numbers from 1-220 were generated without replacement and assigned in order of generation to each section/animal to be sampled. These numbers were then arranged in order from 1-220 for photography. Thus, the order in which sections were photographed was randomized. A summary of the procedures employed for photography appears in Appendix A.

Data collection.

Data were obtained from each negative by placing it on the backlighted table directly underneath the Eyecom II Scanner. In order to keep unwanted table light from entering the Eyecom II, a posterboard template was constructed which entirely covered the light table except for a 2" by 4" portion in the center where the slide was placed.

The image from the negative was then transmitted to the video display terminal where a joystick cursor was used to encircle the area to be sampled. A gray scale frequency distribution was subsequently determined for each sample.

Data from negatives from a single roll of film were collected as a group. Also included on each roll were two frames of neutral density filters which represented two points of the density spectrum (63% and 1% transmittance). These were used to calibrate the camera in order that the gray scale distribution be placed in the same relative

position for each role of film. This compensated for
possible differences in film "batches" and film development.
On each negative a central portion of the SON was sampled
which was interpreted by the Eyecom II system as a frequency
distribution of staining densities. For control purposes, a
portion of the lateral hypothalamic area was also sampled.
Since technical considerations necessitated removal of the
thionine stain, NC was not sampled for this analysis, as it
was not visible without counterstain. From the density
histograms the distributional features of mean, standard
deviation, skewness, and kurtosis, were determined. Data
from sections representing each location within SON were
combined to give a composite distribution representing that
location for each animal. The distributional features
mentioned above were then statistically analysed as the
dependent variables.

Statistical analysis

Data were analysed separately for horizontally and
coronally sectioned brains using a split-plot design for
repeated measures over space (Gill,1978,vol.2).The model for
this design is:

Statistical Model

(Split-Plot design)

$$Y_{ijk} = \mu + \alpha_i + D_{(i)j} + \beta_k + (\alpha\beta)_{ik} + (D\beta)_{(i)jk} + E_{(ijk)}$$

where

α_i = treatment effects (lactation vs. estrus)

$D_{(i)j}$ = random effects of subjects

β_k = effects of location

$(\alpha\beta)_{ik}$ = interactions of treatments with locations

$(D\beta)_{(i)jk}$ = interactions of subjects with location

(Not separable from experimental error).

Analysis of these variables was accomplished with the BMDP statistical package PV2. This program tests the ANOVA assumptions and fills in data for missing cases by calculation of harmonic means. This was necessary for one horizontal control animal as this tissue was lost in processing.

RESULTS

Theoretical considerations.

When morphological changes are induced in astrocytes in vitro by the additon into the medium of dbcAMP, process formation is observed (Kimelburg et al.,1980). If immunostaining for GFAP is done at intervals during process formation, an increasingly higher density staining is produced, which corresponds to filament formation (Trimmer et al., 1979). If a frequency histogram of densities is obtained at the same intervals during the transformation, certain distributional features would be expected to change. Figure 2 illustrates the postulated relationship between the shape of the frequency distribution and the state of the GFAP immunostain.

Methodological controls.

Sample size. The data for sample size are listed in Tables 3a-d, Appendix C. All comparisons of the number of picture elements (pixels) sampled revealed that there were no significant differences in sample size (F<1) for both treatments and locations. This was true in both the horizontal and coronal planes. These data indicate that a relatively consistent sampling of the SON was achieved.

Mean staining density-LHA. Data for the mean staining density of the LHA in coronal section are presented in Table 4b, Appendix C. Analysis of this variable in coronal

Figure 2. Comparing the frequency distribution
characteristics indicates the extent and direction of
changes in staining density. A. Astrocyte prior to the
addition of a process-inducing substance: little GFAP
staining; B. After addition of a process-inducing
substance process formation begins: GFAP staining
increases; C. Process formation complete: intense GFAP
staining.
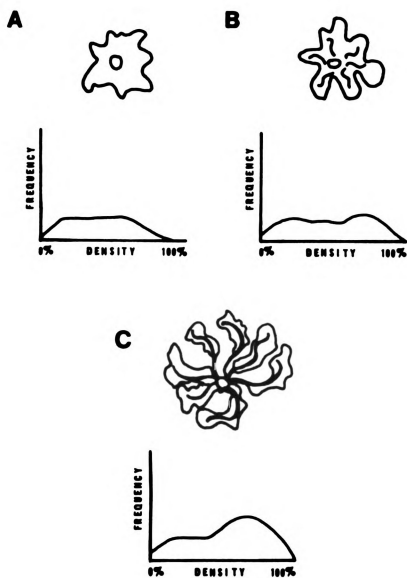
Figure 2.

sections revealed virtually identical mean densities of control and lactating rats in the LHA (Figure 3). Similar results were obtained in horizontal sections (Table 4d, Appendix C). These data indicate successful production of a comparable immunostain in the LHAs of both lactating and control animals.

Tests of treatments, locations, and interactions of treatments with locations.

In order to facilitate the reader's understanding of these results, some interpretations have been included. Differences in mean, standard deviation, skewness and kurtosis have been related to the pattern of the GFAP immunoreactivity which is quantified by these measures.

Mean staining densities: SON. Table 2 lists the data for mean density level of the SON for control and lactating subjects in coronal section (ANOVA Table 4a, Appendix C).

Slit-plot analysis of variance revealed that there were significant differences between control and lactating groups ($p<.05$, $F=8.12$, dfs=1,3) on this measure in coronally sectioned tissue. SONs from lactating rats showed a smaller mean staining density. These data indicate a per unit area reduction in the immunostainable glial cytoskeletal protein. As with all immunological methods, such changes can be related to the availabilty of antigenic sites for binding with the primary antibody. The changes in staining distribution observed here therefore reflect a reduction in available binding sites brought about by a

Figure 3. Graph illustrating the mean staining densities of the SON and LHA in control and lactating subjects. The mean staining density was found to be significantly less in the SONs of coronal lactating animals as compared to controls. No changes were found to occur in the LHA under the same conditions. *=p<.05.
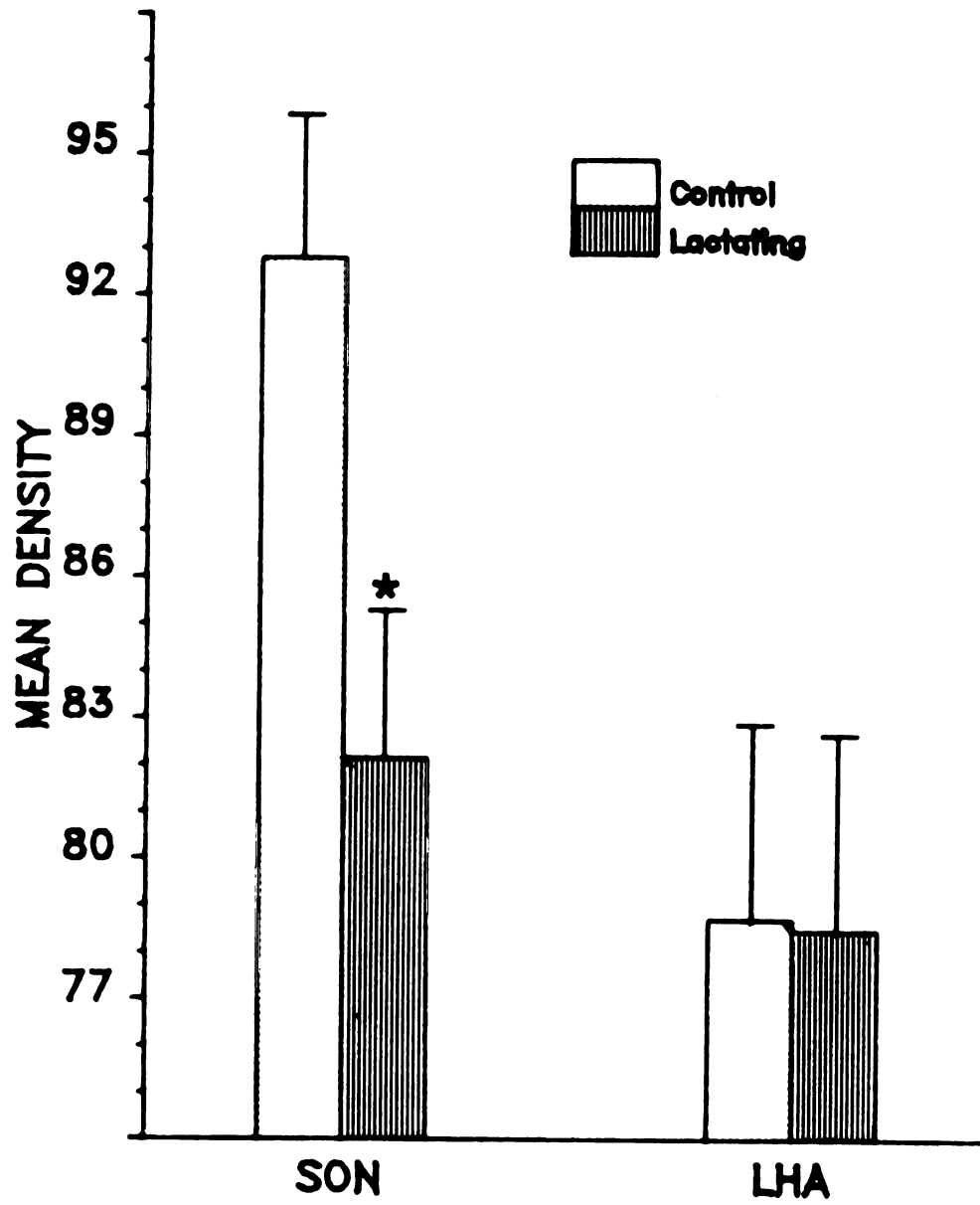
Figure 3.

Table 2. Mean Staining Densities - SON

	Control	Lactating	Location Mean
CORONALS			
Anterior	94.85	81.77	88.30
Posterior	90.75	82.53	86.64
Treatment Mean	92.79	82.15	
Standard Error = ± 2.64			
HORIZONTALS			
Dorsal	93.27	87.16	89.61
Ventral	94.26	90.25	92.02
Treatment Mean	93.76	88.85	
Standard Error = ± 15.64			

change in the configuration of the protein and/or a
reduction in the amount of protein present. One possible
explanation of the per unit area decrease in staining
density is that a few very high density areas have been
formed, that when averaged with an increased low density
area, give an overall lower density rating. However, as
shall be seen with subsequent data, this is not likely to
be the case. Instead, the observed reduction of staining
density probably indicates that the high density regions,
characteristic of those associated with glial processes,
are reduced also. These data are illusrated in Figures
3-9.

In the horizontal plane (Table 2 and Table 4c,
Appendix C), although a trend toward smaller mean density
in lactating animals was apparent, the difference was not
significant ($F=.04$). Standard errors of the mean treatment
effects were $\pm$ 2.64 and $\pm$ 15.64 respectively for coronal
and horizontal sections, indicating a much larger
variabilty in the horizontal plane. No interactions of
locations and treatments were found to be significant
($F=.52$, $F=.08$;coronal and horizontal sections
respectively). Neither were significant differences noted
for locations within the SON ($F=.24$, $F=.28$).
Standard deviation.

Data for the distributional feature of standard
deviation are listed in Tables 5a and b, Appendix C. A

Figure 4. Frequency histogram of GFAP staining densities from subject #91; a ten day lactating animal. A micrograph of the anterior SON of this subject is displayed in figure 5.

Figure 5. Coronal section from the anterior SON of subject #91, a ten day lactating animal. Note that the paucity of staining is confined to the nucleus. Arrows delineate the SON. Higher power micrograph of section shown in figure 8.
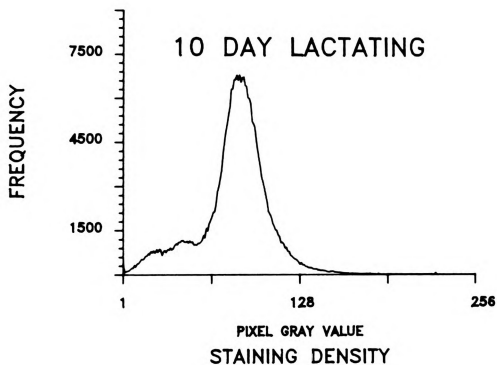
Figure 4.
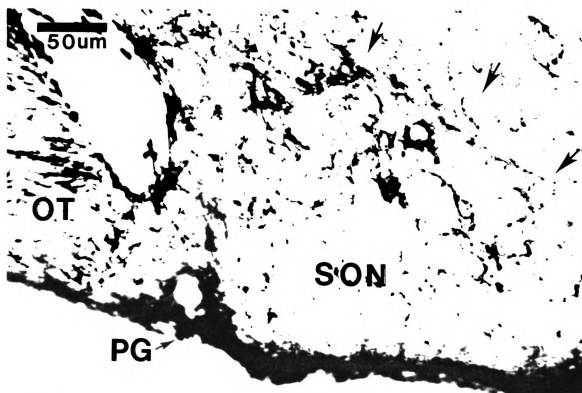
Figure 5.

Figure 6. Frequency histogram of GFAP staining densities from subject #13; a control animal. A micrograph of the anterior SON of this subject is displayed in figure 7.

Figure 7. Coronal section from the anterior SON of subject #13, a control animal. Arrows delineate the SON. Higher power micrograph of section shown in figure 9.
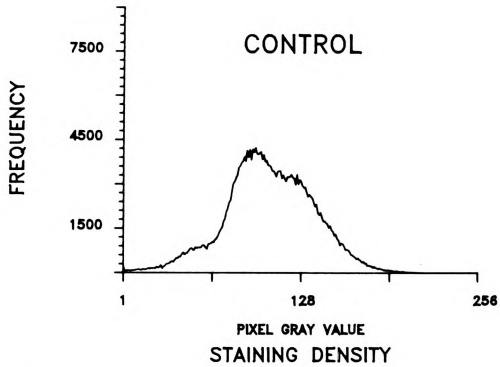
Figure 6.
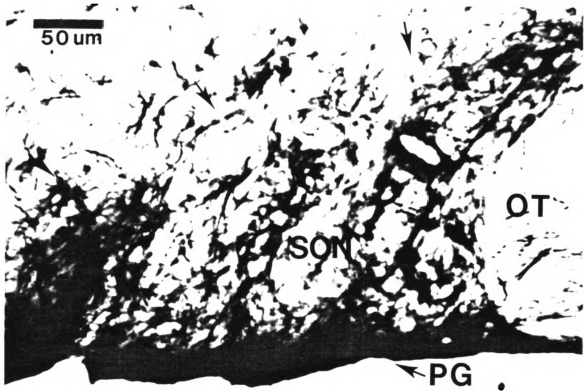
Figure 7.

Figure 8. Lower power micrograph of a section
immunostained for GFAP from a lactating animal. Note the
paucity of staining in the SON and compare to the SON
shown in figure 9.

Figure 9. Lower power micrograph of a section
immunostained for GFAP taken from a control animal. Notice
the dense staining in SON and compare with that in the SON
shown in figure 8.
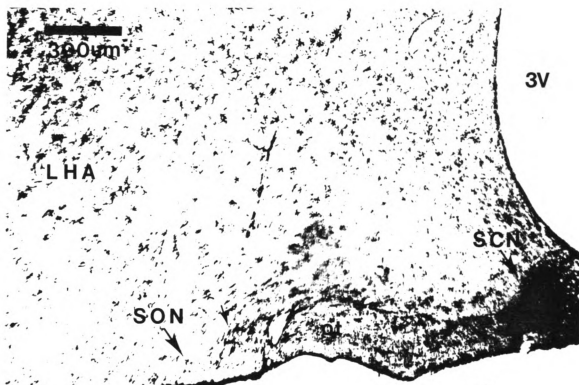
Figure 8.
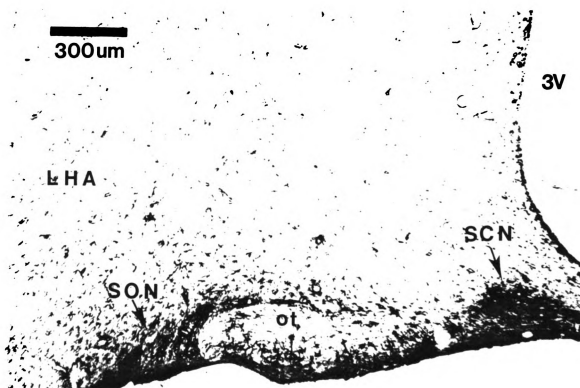
Figure 9.

significant (p,<01, F=14.25, dfs=1,3) difference was found for the location effects within coronally sectioned SONs on this measure. Examination of the mean standard deviation for each location shows that the anterior portion of the control SON has a much greater variabilty of staining densities than does the posterior portion. For this measure, "variability" reflects the frequency with which extreme density values occur. This suggests that the glial protein in the anterior SON exists in a wider range of configurations than it does in posterior SON. Interestingly, a strong trend towards an interaction of treatments with locations was evident in the predominantly oxytocinergic anterior SON (p=.07,F=5.61, dfs=1,3). In control tissue the anterior SON showed a greater variabilty than did posterior SON (Means= 29.9 and 24.1 respectively). However, anterior SON variabilty decreased markedly in lactating animals whereas it stayed constant in the posterior SON. These data can be interpreted as evidence that lactation is accompanied by a morphological homogeneity in the glia of anterior SON. Also, this decrease in variability supports the interpretation that the decreased staining density seen in lactating animals is due to an overall decrease in density, rather than the formation of a few high density areas; as these latter changes would increase the frequency of a wide range of staining densities, i.e., increase variability.

The third moment:skewness.

Data are listed in Tables 6a-d, Appendix C for this variable. The measure of skewness indicates where the majority of immunostaining density values in the distribution are clustered. While not reaching significance, (p=.06, F=8.12, dfs=1,3; p=.09, F=5.65, dfs=1,3) trends were once again noted within the horizontal SON for location and interaction effects respectively. The difference in location effects can be easily observed in Figures 10-13. In control tissue the dorsal SON staining is clustered farther to the left (.735) than are those of the ventral SON (.069). This indicates that more of the area sampled of dorsal SON was less densely stained than in ventral SON. This is precisely what one would expect in the ventral hypothalamus which contains the darkly staining pial-glial plexus. The trends noted for interactions are interesting in that they again demonstrate a regression towards the homogeneity of staining in the lactating animals which was evident on the standard deviation measure. Staining is redistributed to a skew of .425 vs. .364 for dorsal and ventral SON respectively.

The fourth moment.

Data for this measure are displayed in Tables 7a and b, Appendix C. Again, a srong trend (p=.06,F=6.20,dfs=1,3) towards treatment differences for kurtosis, which is a measure of the peakedness of the staining distribution, was observed in coronal SON. Comparisons of the means shows

Figure 10. Densely stained ventral pial-glial plexus, SON.
Horizontal section, control animal.

Figure 11. Dorsal SON from same subject as figure 10.
Horizontal section.
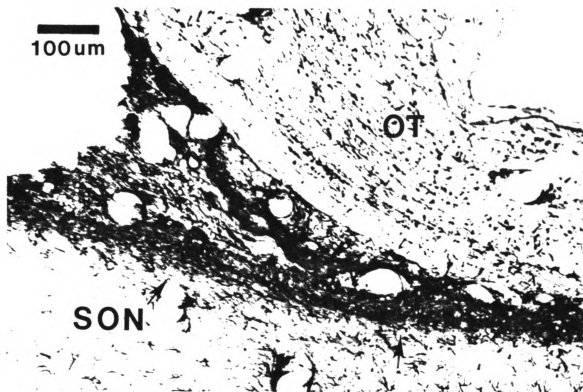
Figure 10.
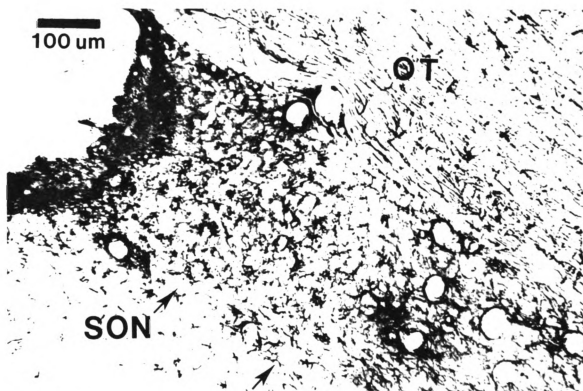
Figure 11.

Figure 12. Densely stained ventral pial-glial plexus, SON. Horizontal section, lactating subject.

Figure 13. Dorsal SON from same subject as figure 12. Horizontal section.
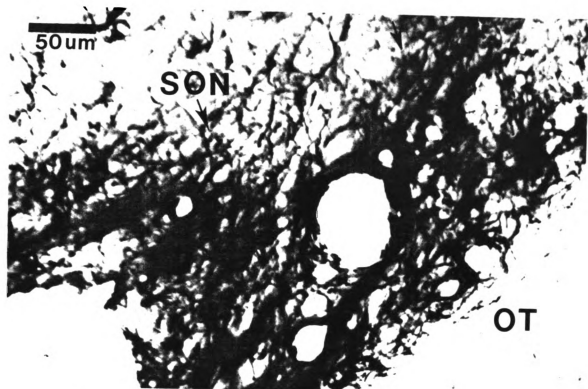
Figure 12.
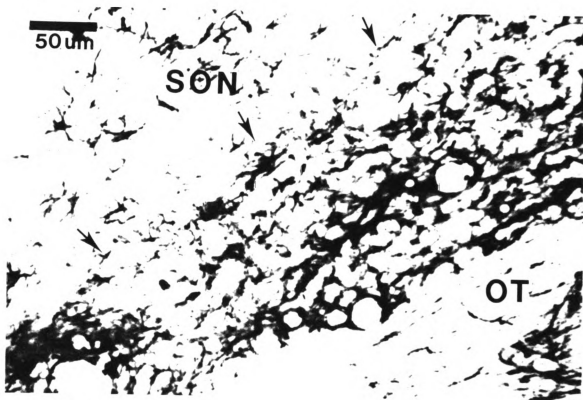
Figure 13.

that the staining distribution is more leptokurtic in the lactating tissue. This is evident in both anterior and posterior SON, but is particularly dramatic in anterior SON, the two portions showing a 1074% and 225% increase over controls respectively. The increased peakedness reflects a decrease in the range of staining densities i.e. more homogeneity of staining.

Summary

Statistical analysis revealed an overall redistribution of GFAP in the supraoptic nucleus of lactating animals. Although observed in all parts of the nucleus, the changes were far more dramatic in the predominantly oxytocinergic portions of the SON. In addition, the changes were to a less dense, more homogeneous distribution of the GFAP, reflective of an absence of high density staining characteristic of that observed in glial processes.

DISCUSSION

The data presented in this report support the view that glia in the SON are capable of altering their morphology during lactation. Although not all of the measures reached conventional levels of statistical significance, the conservative nature of the statistical test which is required by the large number of comparisons made must be considered. In the SON, each significantly and near significantly different measure was congruent with the other to give an overall consistent picture of redistributed GFAP in that nucleus. This was in contrast to the data from the LHA which showed no such redistribution. These results are important for a number of reasons. First, the plasticity of SON glia has been demonstrated _in vivo_. While GFAP redistribution has been shown _in vitro_, it is important to demonstrate that conditions which parallel those of the culture dish exist _in vivo_ as well. Second, the stimulus necessary for inducing this phenomenon was a physiological one: presumably parturition and suckling. Ultrastructural lability of glia has been shown _in vivo_, however it has been induced by CNS insults of various kinds (Maxwell and Kruger, 1965; Harris, 1973; Vaughn and Pease,

1970; and Laursen and Diemer, 1980). With the goal of understanding GFAP's role in neuropathologies, in vitro studies have usually been of cells from pathological tissue, e. g., astrocytomas (Duffy et al.,1982), senile plaques (Duffy et al.,1980), C6 Gliomas (Mares et al., 1981) and Alzheimer's diseased cortex (Schechter et al., 1981). The demonstration of changes in this protein which occur in normal tissue in response to a natural stimulus implies a normal underlying mechanism which somehow has gone awry in pathological tissue. Third, these data provide direct support for the hypothesis that glia actively retract their processes during conditions of high hormone demand. While this phenomenon has been inferred many times in EM studies (LaFarga et al., 1975; Hatton and Tweedle 1980; Hatton and Tweedle,1982; Theodosis et al.,1981;and Tweedle and Hatton;1977) this level of analysis has not provided qualitative evidence that the astrocytes themselves actually change. Finally, these data suggest that the "undifferentiated" state which is often associated with immature astrocytes in culture prior to the addition into the medium of process-inducing subtances, perhaps may be just one of the morphological forms which an astrocyte may assume during its lifetime. An implication of this is that the distinction made between fibrous and protoplasmic astrocytes may actually be functional rather than genomic .

It is illuminating to review recent work by Duffy and coworkers (1982) who have elegantly correlated astrocytic

morphology and plasticity in astrocytic primary cultures.
Using time lapse photography and subsequent immunostaining
for the GFAP, they have shown that the states of greatest
motility are accompanied by a lack of glial processes and
by the presence of a diffuse, homogeneous, distribution of
the GFAP immunostaining. The appearance of a similar
staining distribution in the SON of lactating animals is
consistent with a state of heightened glial motility in
this nucleus during lactation.

The consequence (Tweedle and Hatton,1977) of glial
retraction is to permit a close 6-8 nm apposition between
neurosecretory cells to be formed. It is hypothesized that
these close appositions influence the physiology of the
neurosecretory cells. First, it may allow the formation of
junctional complexes between these cells. Andrew et
al.,(1981) have shown that dye-coupling occurs between
magnocellular cells in vitro in the SON. Recently, it has
been shown that the incidence of dye-coupling between
neurosecretory cells in the paraventricular nucleus in
vitro is influenced by conditions of high hormone demand
(Cobbett and Hatton, submitted). While the relationship of
dye-coupling to the existence of gap junctions is still
controversial, the presence of electrotonic junctions would
provide a means of synchronizing the large number of
oxytocinergic cells which burst simultaneously preceding
milk ejection (Wakerley and Lincoln, 1973). A second way
that glial retraction may influence neurosecretory cells is

by altering the extracellular ionic milieu. It has often
been suggested that astrocytes take up potassium (see Varon
and Somjen, 1979 for review) and it is therefore
conceivable that when cells are active, the absence of glia
would result in raised extracellular potassium, resulting
in an overall increased level of excitabilty of the
neurosecretory cells. Such interaction of closely apposed
neurons has been demonstrated in the cockroach (Yarom and
Spira, 1982).

Computerized image analysis is a technique which
brings precision to the practice of quantifying
immunological and histological staining patterns. It offers
improved resolution, consistency, and objectivity. When
information regarding anatomical distribution is desired,
(i.e. is the GFAP localized to processes or is it
diffused?), this technique offers a clear advantage over
radioimmunoassay. Similar methods have been used (Cowen and
Burnstock,1982) to study changes in the pattern and density
of catacholamine histofluoresence. While the goal of this
study was purely to document relative differences between
groups, Benno and coworkers(1982) have painstakingly
succeeded in correlating (r=.96) immunostaining density
with a biochemical assay.

It is well known that other cytoskeletal proteins are
present in astrocytes, and indeed controversy and confusion
have existed in the literature concerning the similarities
of GFAP, desmin, vimentin, neurofilament, the microfilament

actin, and tubulin (Bigbee and Eng,1982; Bignami et al.,1982; Bray and Gilbert,1981; Ciesielski-Treska et al.,1982,a and b; Dahl et al.,1981,Dahl and Bignami,1982; Geisler et al., 1982; Goldman et al.,1978; Lazarides,1979; Lucas et al.,1980; Reugar et al.,1981; Strocchi et al.,1982; Yen et al.,1976). Suffice it to say, that on the basis of molecular weights, cleavage products, isoelectric variants, tissue of origin, and immunostaining patterns, the possible cross-reactivity of the antiserum used in this study with any of the above proteins is unlikely under the conditions of this experiment. Redistribution of both actin and tubulin, however, has been demonstrated in vitro concurrent with morphological changes of astrocytes (Ciesielski-Treska et al.,1982 a & b.) and the participation of these proteins in glial plasticity cannot be ruled out.

It should be noted that an intriguing exception to the GFAP being localized to neuroectodermally derived astrocytes has recently been found. Hatfield et al.,(submitted) using both immunological and biochemical methods, have demonstrated that GFAP exists in lens epithelium. These authors put forth the suggestion that GFAP may be induced in this ectodermal tissue by functional demands.

The underlying mechanisms which govern the formation and configuration of the GFAP are unknown. An understanding of these processes would undoubtedly shed light on the

influences of glia on the release of neurotransmitters and/or hormones as well as the abberations of the GFAP which have been observed in neuropathologies. In culture preparations, several substances have been shown to induce process formation (Narumi et al.,1978; Tardy et al.,1981) although whether they directly influence the production of GFAP monomer subunits is not clear. Many of these are known to mimic or stimulate adrenergic second messenger systems (Kimelburg et al.,1980; Manthorpe et al.,1979; Moonen et al.,1976; Narumi et al.,1978; Steig et al., 1980). Indeed, astrocyte cultures are routinely used to study adrenergic receptor mechanisms although functional correlates of these cells have not been demonstrated in vivo. It's interesting therefore to consider that the SON is richly innervated by catecholaminergic terminals (Katchachurian and Sladek,1980). Whether these terminals directly affect the morphology of the glia in SON is currently under investigation.

LIST OF REFERENCES

REFERENCES

Andrew, R. D., B. A. MacVicar, F. E. Dudek,and G. I.
    Hatton(1981) Dye-coupling by gap junctions in
    magnocellular neuroendocrine cells of the hypothalamus.
    Science. 211 :1187.

Benno,R.H., L. W. Tucker, T. H. Joh, , and D. J. Reis(1982)
    Quantitative immunocytochemistry of tyrosine hydroxylase
    in rat brain I. Development of a computer assisted
    method using the peroxidase-antiperoxidase technique.
    Brain Res. 246 :225-236.

Bigbee, J. W., and L. F. Eng(1982) Analysis and comparison
    of in vitro synthesized glial fibrillary acidic protein
    with rat CNS intermediate filament proteins. J.
    Neurochem. 38:130-134.

Bignami,A., and D. Dahl(1973) The radial glial of Muller
    and their response to injury. An immunofluorescence
    study with antibodies to the glial fibrillary acidic
    (GFA) protein. Exp. Eye Res. 28 :63-69.

Bignami,A., D. Dahl, and D.C. Reuger (1980) Glial
    fibrillary acidic protein(GFA)iin normal neural cells
    and in pathological conditions. In Advances in Cellular
    Neurobiology vol.1, S. Federoff and L. Hertz, eds., pp.
    285-310 Academic Press, New York.

Bignami,A., T. Raju, and D. Dahl(1982) Localization of
    vimentin, the nonspecific intermediate filament protein,
    in embryonal glia and in early differentiating neurons.
    In vivo and in vitro immunofluorescence study of the rat
    embryo with vimentin and neurofilament antisera.
    Developmental Biology, 91 :286-295.

Bray, D. and D. Gilbert(1981) Cytoskeletal elements in
    neurons. In Ann. Rev. Neurosci.,vol.4,W. M. Cowan,Z. W.
    Hall, and E.R. Kandel,eds.pp.505-523,Annual Reviews
    Inc.,Palo Alto

Ciesielski-Treska,J., B. Guerold, and D. Aunis (1982)
    Immunofluorscence study on the organization of actin in
    astroglial cells in primary cultures. Neuroscience, 7
    :509-522.

Ciesielski-Treska, J., M.-F. Bader, and D. Aunis(1982) Microtubular organization in flat epitheloid and stellate process bearing astrocytes in culture. Neurochemical Research, 7 :275-285.

Cobbett, P. J. R., and G. I. Hatton (submitted) Sex and the coupled neuron: dye coupling in hypothalamic slices under basal and hyperosmotic conditions.

Cowen, T. and G. Burnstock (1982) Image analysis of catecholamine fluorescence. Brain Res. Bull. 9 :81-86.

Dahl D. and A. Bignami(1975)Glial fibrillary acidic protein from normal and gliosed human brain. Demonstration of multiple related polypeptides. Biochimica and Biophysica Acta, 386 :41-51.

Dahl,D. and A Bignami(1977)Effect of sodium dodecyl sulfate on the immunogenic properties of the glial fibrillary acidic protein.J. Immunological Methods, 17 :201-209.

Dahl, D.,D.C. Reuger and A. Bignami(1981)Vimentin, the 57,000 molecular weight protein of fibroblast filaments, is the major cytoskeletal component in immature glia. European Journal of Cell Biology, 24 :191-196.

Dahl,D. and A. Bignami(1982)Immunohistological localization of desmin, the muscle-type 100A filament protein, in rat astrocytes and Muller glia. J. Histochem. Cytochem., 30 :207-213.

DeArmond, S.J., L.F.Eng,and L.J.Rubinstein(1980) The application of glial fibrillary acidic protein immunohistochemistry in neurooncology. A progress report. Path. Res. Pract., 168 :374-394.

Dixon, W. J., and M. B. Brown, eds.(1981) BMDP-81. Biomedical Computer Programs P-Series. University of California Press, Los Angeles.

Duffy,P.E.,L.Graf,and Rapport,M.M.(1978) Immuno-cytochemical diagnoses of brain tumor biopsies. Ann. Neurol. 4 :170.

Duffy,P.E.,L. Graf, and M.M.Rapport (1979) Glial fibrillary acidic protein in ependymomas and other brain tumors:distribution, diagnoses criteria, and relation to differentiation. Neurol. Sci. 40 :113-146.

Duffy,P.E.,M.Rapport, and L. Graf (1980) Glial fibrillary acidic protein and Alzheimer-type senile dementia.Neurology, 30 :778-782.

Duffy, P. E., Y.-.Y. Huang, and M. Rapport (1982) The
    relation of glial fibrillary acidic protein to the
    shape, motility, and differentiation of human
    astrocytoma cells. Experimental Cell Res. 139 :145-157.

Freund-Mercier, M. J., and Ph. Richard(1977) Spontaneous
    and reflex activity of paraventricular nucleus units in
    cycling and lactating rats. Brain Res. 130 : 505-520.

Findley, A. L. R., J. T. Fitzsimmons, and J.
    Kucharczyk(1979) Dependence of spontaneously and
    angiotensin-induced drinking in the rat upon the
    oestrous cycle and ovarian hormones. J. Endocrinol. 82
    :215-225.

Geisler, N., U. Plessman, and K. Weber(1982) Related amino
    acid sequences in neurofilaments and non-neuronal
    intermediate filaments. Nature. 296:448-450.

Gill, J. L. (1978) Design and analysis of experiments.
    Vols. 1 and 2. The Iowa State University Press, Ames.

Goldman, J. E., H. H. Schaumburg, W. T. Norton(1978)
    Isolation and characterization of glial filaments from
    human brain. J. Cell Biol. 78:426-440.

Gregory, W. A., C. D. Tweedle, and G. I. Hatton (1980)
    Ultrasructure of neurons in the paraventricular nucleus
    of normal, dehydrated, and rehydrated rats. Brain Res.
    Bull. 5 :301-306.

Hanakita, J., H. Fumitada, A. Shigera, E. Yamada, and H.
    Handa (1980) Histochemical study on oxidative enzyme
    activity in the brain, particularly of astyrocytes, in
    spontaneously hypertensive rats. Neuropathology and
    Applied Neurobiology. 6 :471-482.

Harris, A. B. (1973) Ultrastructure and histochemistry of
    alumina in cortex. Experimental Neurology. 38 :33-63.

Hatfield, J., R. P. Skoff, and L. Eng. Glial fibrillary
    acidic protein is localized in the lens epithelium.
    (1983) Submitted to Science.

Hatton, G. I., and J. K. Walters (1973)Induced multiple
    nucleoli, nucleolar margination, and cell size changes
    in supraoptic neurons during dehydration and rehydration
    in the rat. Brain Res. 59 :137-154.

Hatton, G. I.(1976) Nucleus Circularis: Is it an
    osmoreceptor in the brain? Brain Res. Bull. 1 :123-131.

Hatton, G. I., and C. D. Tweedle (1980) Suckling increases cell-cell apposition between neurosecretory neurons in the rat supraoptic nucleus. Soc. for Neuroscience Abstracts. 6 :457.

Hatton, G. I., and C. D. Tweedle (1982) Magnocellular neuropeptidergic neurons in hypothalamus:increases in membrane apposition and number of specialized synapses from pregnancy to lactation. Brain Res. Bull. 8 :197-204.

Khachaturian, H. and J. R. Sladek (1980) Simultaneous monoamine histofluorescence and neuropeptide immunocytochemistry :III. Ontogeny of catacholamine varicosities and neurophysin neurons in the rat supraoptic and paraventricular nuclei. Peptides. 1:77-95.

Kimelburg, H. K., S. Narumi, and R. S. Bourke (1978) Enzymatic and morphological properties of primary rat brain astrocyte cultures, and enzyme development in vivo. Brain Res. 153 :55-77.

LaFarga, M., G. Palacios, and R. Perez (1975) Morphological aspects of the functional synchronization of supraoptic neurons. Experientia. 31 :348-349.

Landis, M. D., and T. S. Reese (1981) Astrocyte membrane structure:changes after circulatory arrest. J. Cell Biol. 88 :660-663.

Latov, N., G. Nilaver, E. A. Zimmerman, W. C. Johnson, A. J. Silverman, R. Defendini, and L. Cote (1979) Fibrillary astrocytes proliferate in response to brain inury. Developmental Biology, 72 :381-384.

Laursen, H., and N. H. Diemer (1980) Morphometry of astrocyte and oligodendrocyte ultrastructure after portocaval anastomosis in the rat. Acta Neuropathology(Berl) 51 :65-70.

Lazarides, E.(1980) Intermediate filament proteins as integrators of cellular space. Nature. 283 :249-256.

Liem, R. (1982) Simultaneous separation and purification of neurofilament and glial filament proteins from brain. J. Neurochem. 38 :142-150.

Lucas, C. V., K. G. Bensch, and L. F. Eng (1980) In vitro polymerization of glial fibrillary acidic (GFA) protein extracted from multiple sclerosis (MS) brain. Neurochemical Research. 5 :247-254.

Lucas, C. V., E. P. Reaven, K. G. Bensch, and L. F. Eng (1980) Immunoperoxidase staining of glial fibrillary acidic (GFA) protein polymerized in vitro: an ultramicroscopic study. Neurochemical Research. 5:1199-1209.

Manthorpe, M., R. Adler, and S. Varon (1979) Development, reactivity and GFA immunofluorescence of astroglia-containing monolayer cultures from rat cerebrum. J. Neurocytol. 8 :605-621.

Mares, V., V. Fleischmannova, Z. Lodin, and H. Ueberberg(1981) Cyclic AMP and growth regulation in rat glioma cells in tissue culture. Experimental Neurology. 71:154-160.

Moonen, G., E. Heinen, and Goessens, G. (1976) Comparative ultrastructural study of the effects of serum-free medium and dibutyrl cyclic AMP on newborn brain astroblasts. Cell Tiss. Res. 167:221-227.

Maxwell, D. S., and L. Kruger (1965) The fine structure of astrocytes in the cerebral cortex and their response to focal injury produced by heavy ionizing particles. J. Cell Biol. 25:141-157.

Narumi, S. H., K. Kimelburg, and R. S. Bourke (1978) Effects of norepinephrine on the morpholgy and some enzyme activities of primary monolayer cultures from rat brain. J. Neurochem. 31:1497-1490.

Negoro, H., S. Vissessuwans, and R. C. Holland (1973) Reflex activation of paraventricular nucleus units during the reproductive cycle and in ovariectomized rats treated with oestrogen or progesterone. J. Endocrinol. 59 : 559-567.

Nequin, L. G., J. Alvarez, and N. B. Schwartz (1979) Measurement of serum steroid and gonadotropin levels and uterine and ovarian variables throughout four-day and five-day estrous cycles in the rat. Biology of Reproduction. 20:659-670.

Paterson, J. A., and C. P. LeBlond (1977) Increased proliferation of neuroglia and endothelia cells in the supraoptic nucleus and hypophysial neural lobe of young rats drinking hypertonic sodium chloride solution. J. Comp. Neurol. 175:373-390.

Pertti, A., H. von Kuskull, K. Teramo, O. Karjalainen, I. Virtanen, V.-P. Lehto, and D. Dahl (1980) Glial origin of rapidly adhering amnionic fluid cells. British Medical Journal. 28:1-5.

Picker, S., and S. Goldring (1982) Electrophysiological properties of human glia. Trends in Neuroscience. 45:73-76.

Rhodes, C. H., J. I. Morrell, and D. W. Pfaff (1981) Distribution of estrogen concentrating, neurophysin-contaning magnocellular neurons in the rat hypothalamus as demonstrated by a technique combining steroid autoradiography and immunohistology in the same tissue. Neuroendocrinology. 33:18-23.

Rueger, D. C., E. E. Gardner, H. Der Simonian, D. Dahl, and A. Bignami (1981)Purified glial fibrillary acidic protein and desmin are distinct intermediate filament proteins exhibiting similar properties.J. Biological Chemistry. 256:10606-10612.

Salm, A. K., and G. I. Hatton (1980) An immunocytochemical study of astrocytes associated with the rat supraoptic nucleus. Soc. for Neuroscience Abstracts. 6:547.

Sar, M., and W. E. Stumpf (1980) Simultaneous localization of [3-H] estradiol and neurophysin I or arginine vasopressin in hypothalamic neurons demonstrated by a combined technique of dry-mount autoradiography and immunohistochemistry. Neuroscience Letters. 17:179-184.

Sar, M., and W. E. Stumpf (1981) Combined autoradiography and immunohistchemistry for simultaneous localization of radioactively labeled steroid hormones and antibodies in the brain. J. Histochem. Cytochem. 29:161-166.

Schachner, M., T. E. Hedley-Whyte, D. W. Hsu, G. Schoonmaker, and A. Bignami (1977) Ultrastructural localization of glial fibrillary acidic protein in mouse cerebellum by immunoperoxidase labelling. J. Cell Biol. 75:67-73.

Schechter, R., C. Y. Shu-Hui, and R. D. Terry (1981) Fibrous astrocytes in senile dementia of the Alzheimer type. J. Neuropathol. Exptl. Neurol. XL:95-101.

Skowsky, W. R., L. Swan, and P. Smith (1979) Effects of sex steroid hormones on arginine vasopressin in intact and castrated male and female rats. Endocrinology. 104:105-108.

Smithson, K. G., B. A. MacVicar, and G. I. Hatton (1983) Polyethylene glycol embedding: A technique compatible with immunocytochemistry, enzyme histochemistry, histofluorescence and intracellular staining. J. Neuroscience Methods. 7:27-41.

Sternberger, L. A. (1974) Immunocytochemistry. Foundations of Immunology Series. pp129-171, Prentice Hall, Inc. New Jersey.

Steig, P. E., H. K. Kimelberg, J. E. Mazurkiewicz, and G. A. Banker (1980) Distribution of glial fibrillary acidic protein and fibronectin in primary astroglial cultures from rat brain. Brain Res. 199:493-500.

Strocchi, P., D. Dahl, and J. M. Gilbert (1982) Studies on the biosynthesis of intermediate filament proteins in the rat CNS. J. Neurochem. 39:1132-1141.

Swaab, D. F., and J. F. Jongkind (1970) The hypothalamic neurosecretory activty during the oestrus cycle, pregnancy, parturition, lactation, persistent oestrus, and after gonadectomy, in the rat. Neuroendocrinology. 6:133-145.

Tardy, M., C. Fages, B. Rolland, J. Bardakdjian, and P. Gonnard (1983) Effects of prostglandins and dibutyrl cyclic AMP on the morphology of cells in primary astroglial cultures and on metabolic enzymes of GABA and glutamate metabolism.Experientia. 37:19.

Theodosis, D. T., D. A. Poulain, and J.-.D. Vincent (1981) Possible morphological basis for synchronisation of neuronal firing in the rat supraoptic nucleus during lactation. Neuroscience. 6:919-929.

Trimmer, P., P. Reier, and T. Oh (1980) Morphological studies of normal and induced astrocytic differentiation in vitro. Neuroscience Abstracts. 6:291.

Tweedle, C. D., and G. I. Hatton (1976) Ultrastructural comparisons of neurons of supraoptic and circularis nuclei in normal and dehydrated rats. Brain Res. Bull. 1:103-121.

Tweedle, C. D.,and G. I. Hatton (1977) Ultrastructural changes in rat hypothalamic neurosecretory cells and their associated glia during minimal dehydration and rehydration. Cell Tiss. Res. 181:59-72.

Tweedle, C. D., and G. I. Hatton (1980a) Evidence for dynamic interactions between pituicytes and neurosecretory axons in the rat. Neuroscience. 5:661-667.

Tweedle, C. D., and G. I. Hatton (1980b) Glial cell enclosure of neurosecretory endings in the neurohypophysis of the rat. Brain Res. 192:555-559.

Tweedle, C. D., and G. I. Hatton (1982) Magnocellular neuropeptidergic terminals in neurohypophysis: Rapid glial release of enclosed axons during parturition. Brain Res. Bull. 8:205-209.

Vaughn, J. E., and Pease (1970) Electron microscopic studies of Wallerian degeneration in rat optic nerves. J. Comp. Neurol. 140:207-226.

Varon, S. S., and G. G. Somjen (1979) Neuron-glia interactions. Neuroscience Research Program Bulletin. #17.

Virchow, R.(1840)Cellular Pathology. Trans. from the second German edition by F. Chance. London, Churchill. pp272-280. As cited in The Fine Structure of the Nervous System. The neurons and supporting cells.A. Peters, S. L. Palay, and H. Webster eds. (1976) W. B. Saunders Co., Philadelphia.

Wakerley, J. B., and D. W. Lincoln (1973) The milk ejection reflex of the rat: A 20-40 fold acceleration in the firing of paraventricular neurones during oxytocin release. J. Endocrinol. 57:477-493.

Watson, W. E. (1971) Some metabolic responses of rat neuroglial cells to perfusion of the cerebral ventricles with artificial cerebrospinal fluid of abnormal composistion. J. Physiol. 218:88-89P.

Watson, W. E.(1972) A quantitative study of some neuroglial responses to neuronal stimulation. J. Physiol.(Lond.)225 : 54-55P.

Weber, K., and M. Osborn (1969) The reliabilty of molecular weight determinations by dodecyl sulfate-polyacrylamide gel electrophoresis. J. Biological Chemistry. 224:4406-4412.

Yarom, Y., and M. E. Spira(1982) Extracellular potassium
    ions mediate specific neuronal action. Science.
    216:80-82.

Yen, S.-H., D. Dahl, M. Schachner, and M. L.
    Shelanski(1976) Biochemistry of the filaments of brain.
    Proc. Nat. Acad. Sci. 73:529-533.

APPENDIX A

APPENDIX A

Protocols

Immunostaining Pretreatment

 1) 5% hydrogen peroxide, 1/2 hour

 2) TBS rinse 2X, 10 minutes

 3) .1M sodium periodate, 15 minutes

 4) TBS rinse 3X, 15 minutes

 5) Sodium borohydride (10mg/ml), 10 minutes

 6) TBS rinse 4X, 20 minutes

 7) 5% dimethylsulfoxide (DMSO), 10 minutes

 8) TBS rinse 2X, 10 minutes

 9) 10% normal goat serum in TBS

10) Remove normal goat serum. Briefly rinse.

Immunocytochemistry Protocol

 1) Primary anti-GFAP, 16 hours @4°C., 1:1500 in TBS

 2) TBS rinse, 1 hour

 3) Goat anti-rabbit serum, 1.5 hours @ 4°C., 1:50 in TBS

 5) Peroxidase-antiperoxidase, 1.5 hours, 1:350 in TBS

 6) TBS rinse, 4X in 2 hours

 7) Glucose-oxidase reaction, 5 minutes

 8) TBS rinse 3X

All steps contain <1% triton-X 100

APPENDIX A

Protocols

Glucose Oxidase Reaction for Imunocytochemistry

(room temperature)

To 200 mls of .15M Phosphate Buffer pH 7.2 add:

    100 mg DAB

    Filter solution through .22 um filter

Add:

    400 mg Beta-D(+) glucose

    80 mg ammonium chloride

    .6 mg Glucose Oxidase Type VII

Incubate section in this solution until brown reaction product forms. For smaller quantities of the final reaction solution, aliquots from previously mixed and frozen DAB - buffer and glucose oxidase solutions can be combined.

EM-Immuno Fixative

1% glutaraldehyde

2.5% paraformaldehyde

      in

.1M cacodylate buffer, pH 7.25

Dissolve 21.4 g Na cacodylate in 800 ml double distilled water in a 1l beaker. Adjust pH to 7.25

Add 40 ml of stock 25% glutaraldehyde

Rinse twice with distilled water

APPENDIX A

Protocols

Add 125 ml of stock 20% paraformaldehyde

Transfer with three rinses to liter volumetric and Q.S.

Note: HCl + formalin forms carcinogenic fumes.

Pretreatment Solutions (in Tris Buffered Saline)

1)   .1M Sodium periodate = 21.39g/liter = 2.139g/100mls

solution

2)   Sodium borohydride (10mg/ml) = 500mg/50mls solutionn

3)   5% DMSO = 5mls/100mls solution

4)   5% hydrogen peroxide = 15mls 30% H_2O_2 /90mls soln

5)   10% normal goat = 5mls serum/50mls solution

TBS- Tris Buffered Saline

pH 7.6 @ 25 C

Measure following chemicals and transfer to a liter beaker

1.   6.06 g. Tris HCL

2.   1.39 g. Tris base

Adjust pH to 7.6 with appropriate acid or base solutions

3.   8.7 g. NaCl

Transfer with three rinses to a liter volumetric

Q.S. to the mark and stir vigorously.

APPENDIX A

Protocols

<u>TBS-Tris</u> <u>Buffered</u> <u>Saline</u>

pH 7.6 @ 5 <u>C</u>

Measure the following chemicals and transfer to a 500 ml

beaker

1.   3.595 g. Tris HCl

2.   .250 g. Tris base

Adjust pH to 7.1 with appropriate acid or base solutions

3.   4.350 g. NaCl

Transfer with three rinses to a 500 ml volumetric

Q.S. to the mark and stir vigorously.

APPENDIX A

Protocols

<u>Procedure</u> <u>for</u> <u>Thionine</u> <u>Staining</u>

1) Xylene 10 - 15 min

2) 100% ETOH 5 min

3) 95% ETOH 2 min

4) 70% ETOH 2 min

5) Distilled water 5 min

6) Thionine stain

7) Distilled water 1 min

8) 70% ETOH 30 - 60 sec

9) 95% ETOH differentiate

10) 100% ETOH 3 min

11) Xylene 1X 5 min

12) Xylene 2X 10 min

13) Cover slip

Thionine= .5% in .2M Acetate buffer, pH 5.0

APPENDIX A

Protein purification.

Protein was isolated from human postmortem cerebral white matter with the procedure described by Dahl and Bignami (1977). Briefly, tissue was extracted in .01M sodium phosphate buffer, pH 6.2 at 4 degrees C. Further extraction was done in 0.05M phosphate buffer. This homogenate was then centrifuged at 12,000 X g or 100,000 X g.

The GFAP was then absorbed to hydroxylapitite in 0.05M sodium phosphate buffer prior to elution of GFAP with 0.01M potassium phosphate, pH 8.0. Eluates positive by immunodiffusion were pooled and precipitated with saturated ammonium sulfate (Dahl and Bignami, 1975). Further purification was achieved by extraction from sodium dodecyl sulfate polyacrylamide gels following electrophoresis (Dahl and Bignami, 1977; Weber and Osborn, 1969).

Antiserum production and method specificity. Antibodies were produced over a period of six months by multiple backsite injections of a total of 1mg GFAP in Freund's adjuvant. When tested with GFAP in an Ouchterlony double immunodiffusion plate, the antiserum yielded a single precipitin line.

APPENDIX A

Protein purification-cont.

Method specificity was tested on sections adjacent to those processed normally by ommission of the primary antiserum or substitution of preimmune serum for the primary antiserum. Both procedures resulted in an abolition of staining.

Image analysis hardware/software.

The imaging system consists of 1) a TV camera, 2) Eyecom Image Scanner with a B/W TV monitor, 3) Datacolor Edge Enhancer, 4) B/W TV monitor on a 108 pt. terminal, and 5) a color TV monitor. All these components are made by Spatial Data Systems, Goleta, Ca. The terminal is interfaced with a PDP-11/34 computer. Images are transmitted to the Eyecom Scanner from photographs or negatives placed on a tungsten illuminated backlighted table. For the present project, the latter method, using black and white negatives was chosen. The image is digitized and displayed, slightly magnified, on the terminal screen consisting of (480 X 640) 307,200 picture elements (PIXELS). The system is capable of assigning one of 256 gray level designations based upon the amount of light transmitted through the negative to each pixel. The distribution of gray levels present in any one image can then be displayed as a frequency histogram.

APPENDIX A

Optical equipment: 1) Zeiss microscope with a
tungsten halogen light source, 2) Zeiss 10X planapo
objective with anumerical aperature of .32 and a 5.5um
depth of field, 3) Zeiss achromatic, aplanatic, substage
condenser, numerical aperature = 1.4, 4) #1.5 coverslips (
.16mm to .19mm thick).

The condensers were adjusted to give modified Kohler
illumination in order to increase contrast and optimize
resolution. For photography, the image was directed down a
mechanical tube containing a 0.5X lens to a Nikkormat
camera. The optimum wavelengh attainable with this sytem
is .32um.

Photography procedures:

1) Check batteries in the light meter and camera.

2) Check all lenses and glass for dirt: clean as
necessary.

3) Load film.

4) Put on eyeglasses and focus Nikon eyepiece reticule.

5) Select slide and clean as necessary.

6) Find desired section through Nikkormat eyepiece,
compose picture, focus.

7) Close down field diaphragm and focus it with substage
condenser.

8) Open field diaphragm far enough to illuminate field as
seen through eyepiece. (This was determined to be position
11 and remained constant thereafter).

APPENDIX A

Photography procedures-cont.

9) See a piece of dirt on the image, curse, reclean slide and/or lenses as necessary.

10) Repeat steps 7, 8, but not 9 if lucky.

11) Move slide so that only Permount is visible thru eyepiece. Use lightmeter to adjust light to 6uA. Return slide to original position.

12) Refocus through eyepiece and reshoot picture.

If not beginning a role of film steps 5-12 were followed prior to each shot. If beginning a role of film additional steps were followed:

(10a. Remove slide.

    b. Adjust light to 6uA through eye piece.

    c. Place a #2 neutral density filter (1% light transmittance) on the field diaphragm and take picture.

    d. Repeat step C using a #0.2 neutral density filter (63% light transmittance).

      Thus each roll of film had frames corresponding to 1% and 63% light transmittance. (The neutral density filters were generously loaned by Dr. James Zachs). Photomicrographs of a stage micrometer were taken for later focussing of the TV camera and determination of magnification.

      From prior tests it was empirically determined that an ASA setting of 25 and a shutter speed of 1/250th of a second, in combination with the light level previously

APPENDIX A

Photography procedures-cont.

 described and specific development parameters, produced a
(slightly underexposed) negative which rendered maximal
detail of immunostain.

    Small tank film development. Dilution D (1:9) of
Kodak's HC-110 developer was used for 8 minutes at 68
degrees F with agitation every 30 seconds. Following
development, stop bath (30 seconds) and then fixer (4
minutes) were added to the tank. A 15 minute wash and then
application of photo-flo finished the process. Dried
negatives were mounted in a Pakon or Soligar slide binder.

APPENDIX B

APPENDIX B

Supplies and equipment

Image Analysis Equipment

Source: Spatial Data Systems

P.O. Box 249

Goleta, CA   93017

(1977

prices)

Combination Data Color System with Eyecom picture terminal and I/O controller for PDP/11	$31,400.00
Refresh Memory Planes	850.00
32 Color Output Board	950.00
PDP/11 Routines for console table and Camera table	1,000.00
Density readout for model 401/704	600.00
Polaroid camera system	800.00
	$38,900.00
Educational Discount	1,945.00
	$36,955.00

APPENDIX B

Supplies and equipment

Supply	Source	#	Cost

Tris Buffered Saline

Supply	Source	#	Cost
Trizma Base	Sigma	500 g	$14.25
Trizma Hydrocholoride	Sigma	500 g	26.10
Sodium Chloride	Mallinckrodt	1 lb	1.77
Triton- X 100	Mallinckrodt	500 ml	3.40
Buffer Standard Soln. pH 7.00	Mallinckrodt	1 pt	1.47

Glucose-Oxidase Reaction

3,3' -Diaminobenzidine Tetrachloride Grade II

Supply	Source	#	Cost
	Sigma	5 g	12.50
Ammonium Chloride	Mallincrodt	1 lb	1.93
B - D(+) glucose	Sigma	10 g	2.50
Glucose Oxidase Type VII	Sigma	10,000 units	7.15

Immunocytochemical Pretreatment

Supply	Source	#	Cost
Sodium meta-Periodate	Sigma	25 g	4.75
Sodium Borohydride	Sigma	25 g	5.30
30% Hydrogen Peroxide	Mallinckrodt	1 pt	2.31
Normal goat serum	Antibodies Inc.	ml	2.31
Dimethyl Sulfoxide	Mallinckrodt	pt	5.53
37% Hydrochloric Acid	Mallinckrodt	6 lb/btl	4.70

APPENDIX B

Supplies and equipment

Supply	Source	#	Cost
20% Aqueous			
EM Grade Paraformaldehyde	Polyscience	1 pt	$11.55
Sodium Cacodylate	Polyscience	50 g	20.00
Goat anti-rabbit gamma			
globulin P4	Antibodies Inc.	ml	5.35
Normal goat serum	Antibodies Inc.		
		20 ml	5.00
Permount	Fisher Sci.	500 ml	10.25
95% EtOH	MSU Stores	1 gal	3.40
Xylene	MSU Stores	5 gal	13.64
25% glutaraldehyde	EM Science	1 pt	6.00
Gelatin	MSU Stores	1 lb	7.80

Equipment

Spinbar-Teflon	Biochemistry Stores		
8 x 1.5 mm		1	1.13
15 x 1.5 mm		1	1.43
3 x 1/2 in.		1	3.43
Latex gloves		1	1.10
Surgeon's gloves		1	.65
Parafilm		1 roll	6.53
Weighboats		500	18.96

APPENDIX B

Supplies and equipment

Equipment	Source	#	Cost
Pipet bulbs		1 pk	$2.18
Test tube support		1	3.93
Corning coverslips #1		1 pk	5.26
1 cc syringes		100	12.88
Disposable needles		100	8.80
Falcon tubes		case	63.35
Corning magnetic stirrer			85.00

Filter System

Equipment	Source	#	Cost
.45 um filter, triton free	Millipore	100	34.40
13 mm filter holder		10	23.70
13 mm gasket		100	15.40
.22 um filter, triton free		100	31.00
25 mm filter holder		12	47.60
25 mm gasket		100	31.20
milli-RO4		1	1513.00
Rogard prefilter		1	85.50
Carbon cartridge			116.00
RO cartridge		1	419.00
ion exchange cartridge		2	70.00
Milli Q		1	1795.00

APPENDIX B

Supplies and equipment

Equipment	Source	#	Cost
Pump motor		1	191.00
Reservoir			712.00

APPENDIX C

APPENDIX C

Key to ANOVA and Cell Mean Tables

Type:.......Effects due to hormonal state, i.e., lactation
verses estrus.

Place:.....Effects due to location within the SON, i.e.,
anterior verses posterior or dorsal verses
ventral.

Pt:........Effects due to interaction of place (location)
with type (hormonal state) variables.

Marginal:..Means for each subgroup.

Count:.....Number of subjects in group.

See BMDP-81, Dixon and Brown, eds. (1981), for further
reading.

APPENDIX C

Table 3a. ANOVA table-sample size-Coronal SON

SOURCE	SS	DEGREES OF FREEDOM	MEAN SQUARE	F	TAIL PROB.
MEAN				309.51	.0001
TYPE	1219055050.08	1	1219050505.08	.50	.5184
ERROR	9745250020.66	4	2436312505.16		
PLACE	150343802.08	1	150343802.08	.05	.8297
Pt	2316991252.08	1	2316991252.08	.81	.4185
ERROR	11416441453.33	4	2854111370.83		

APPENDIX C

Table 3b. ANOVA Table-Sample size-Coronal LHA

SOURCE	SS	DEGREES OF FREEDOM	MEAN SQUARE	F	TAIL PROB.
MEAN		1		1455.87	.0000
TYPE	22029590.08	1	22029590.08	.00	.9691
ERROR	51915515704.16	4	12978878926.16		
PLACE	190937474.08	1	190937474.08	.01	.9262
Pt	154304510.08	1	154004510.08	.01	.9337
ERROR	78650833563.33	4	19662708390.83		

APPENDIX C

Table 3c. ANOVA table-Sample size-Horizontal SON

SOURCE	SS	DEGREES OF FREEDOM	MEAN TAIL SQUARE	F	PROB.
MEAN		1		93.14	.0024
TYPE	20878004497.06	1	20878004497.06	2.30	.2270
ERROR	27284657193.33	3	9094885731.11		
PLACE	254278272.06	1	254278272.06	.04	.8465
Pt	5396737424.06	1	5396737424.06	.94	.4028
ERROR	17145206984.33	3	5715068994.77		

APPENDIX C

Table 3d. ANOVA Table-Sample Size-Horizontal LHA

SOURCE	DEGREES OF SS	MEAN FREEDOM	TAIL SQUARE	F	PROB.
MEAN		1		248.80	.0006
TYPE	20750272246.81	1	20750272246.81	1.45	.3143
ERROR	42801488388.58	4	14267162796.19		
PLACE	2948139626.01	1	2948139626.01	4.03	.1384
Pt	6759186254.01	1	6759186254.01	9.24	.0559
ERROR	2195362084.58	3	731787361.52		

APPENDIX C

Table 4a. ANOVA Table-Mean Density-Coronal SON

SOURCE	SS	DEGREES OF FREEDOM	MEAN SQUARE	F	TAIL PROB.
MEAN	91823.64	1	91823.64	2103.79	.0000
TYPE	339.71	1	339.71	8.71	.0464
ERROR	167.42	4	41.85		
PLACE	8.33	1	8.33	.24	.6482
Pt	17.74	1	17.74	.52	.5122
ERROR	137.44	4	34.36		

APPENDIX C

Table 4b. ANOVA Table-Mean Density-Coronal LHA

SOURCE	SS	DEGREES OF FREEDOM	MEAN SQUARE	F	TAIL PROB.
MEAN	74127.74	1	74127.74	979.37	.0000
TYPE	.18	1	.18	.00	.9632
ERROR	312.75	4	75.68		
PLACE	1.24	1	1.24	.01	.9210
Pt	1.24	1	1.24	.01	.9209
ERROR	446.97	4	111.74		

APPENDIX C

Table 4c. ANOVA Table-Mean Density-Horizontal SON

SOURCE	SS	DEGREES OF FREEDOM	MEAN SQUARE	F	TAIL PROB.
MEAN	80030.95	1	80030.95	54.50	.0051
TYPE	58.02	1	58.02	.04	.8551
ERROR	4405.62	3	1468.54		
PLACE	11.39	1	11.39	.28	.6334
Pt	3.37	1	3.37	.08	.7921
ERROR	122.05	3	40.68		

APPENDIX C

Table 4d. ANOVA Table-Mean Density-Horizontal LHA

SOURCE	SS	DEGREES OF FREEDOM	MEAN SQUARE	F	TAIL PROB.
MEAN	55465.83	1	55465.83	156.41	.0011
TYPE	4.18	1	4.18	.01	.9211
ERROR	1063.86	3	354.61		
PLACE	18.34	1	18.34	.16	.7181
Pt	25.37	1	25.37	.22	.6725
ERROR	348.57	3	116.52		

APPENDIX C

Table 4e. Cell Means and Standard Deviations for Mean
Density-Coronal LHA

Cell Means

	CONTROL	LACTATING	MARGINAL
ANTERIOR	71.718	79.116	78.917
POSTERIOR	78.719	77.828	78.273
MARGINAL	78.719	78.472	78.595
COUNT	3	3	6

Standard Deviations

	CONTROL	LACTATING
ANTERIOR	9.219	14.477
POSTERIOR	8.211	3.557

APPENDIX C

Table 4f. Cell Means and Standard Deviations for Mean
Density-Horizontal SON

	Cell Means		
	CONTROL	LACTATING	MARGINAL
DORSAL	93.266	87.164	89.605
VENTRAL	94.259	90.528	92.020
MARGINAL	93.763	88.846	90.813
COUNT	2	3	5

Standard Deviations

	CONTROL	LACTATING
DORSAL	34.611	26.575
VENTRAL	36.931	16.632

APPENDIX C

Table 5a. ANOVA Table-Standard Deviation-Coronal SON

SOURCE	SS	DEGREES OF FREEDOM	MEAN SQUARE	F	TAIL PROB.
MEAN	8147.21	1	8147.21	2358.97	.0000
TYPE	11.19	1	11.19	3.26	.1455
ERROR	13.75	4	3.43		
PLACE	39.56	1	39.56	14.25	.0195
Pt	15.57	1	15.57	5.61	.0770
ERROR	11.11	4	2.77		

APPENDIX C

Table 5b. Cell Means and Standard Deviations for Standard
Deviation-Coronal SON

Cell Means

	CONTROL	LACTATING	MARGINAL
ANTERIOR	29.977	25.757	27.872
POSTERIOR	24.067	24.41	24.240
MARGINAL	27.022	25.090	26.058
COUNT	3	3	6

Standard Deviations

	CONTROL	LACTATING
ANTERIOR	1.317	1.160
POSTERIOR	1.457	2.661

APPENDIX C

Table 6a. ANOVA Table-Skewness-Horizontal SON

SOURCE	SS	DEGREES OF FREEDOM	MEAN SQUARE	F	TAIL PROB.
MEAN	1.52	1	1.52	8.90	.0584
TYPE	.00	1	.00	.00	.9788
ERROR	.51	3	.17		
PLACE	.31	1	.31	8.12	.0651
Pt	.22	1	.22	5.65	.0978
ERROR	.11	3	.03		

APPENDIX C

Table 6b. Cell Means and Standard Deviations for Skewness-
Horizontal SON

Cell Means

	CONTROL	LACTATING	MARGINAL
DORSAL	.73586	.42507	.54938
VENTRAL	.06952	.36492	.24676
MARGINAL	.40269	.39499	.39807
COUNT	2	3	5

Standard Deviations

	CONTROL	LACTATING
DORSAL	.41752	.27905
VENTRAL	.54427	.05105

APPENDIX C

Table 6c. ANOVA Table-Skewness-Horizontal LHA

SOURCE	SS	DEGREES OF FREEDOM	MEAN SQUARE	F	TAIL PROB.
MEAN	1.88	1	1.88	9.97	.0510
TYPE	.81	1	.01	.09	.7822
ERROR	.57	3	.19		
PLACE	.30	1	.30	2.78	.1942
Pt	1.28	1	1.28	11.65	.0422
ERROR	.33	3	.11		

APPENDIX C

Table 6d. Cell Means and Standard Deviations for Skewnesss - Horizontal LHA

Cell Means

	CONTROL	LACTATING	MARGINAL
DORSAL	.94742	.29972	.55880
VENTRAL	-.14355	.67434	.34919
MARGINAL	.40194	.48703	.45299
COUNT	2	3	5

Standard Deviations

	CONTROL	LACTATING
DORSAL	.87824	.06012
VENTRAL	.12820	.23259

APPENDIX C

Table 7a. ANOVA Table-Kurtosis-Coronal SON

SOURCE	SS	DEGREES OF FREEDOM	MEAN SQUARE	F	TAIL PROB.
MEAN	6.32	1	6.32	23.10	.0086
TYPE	1.69	1	1.69	6.20	.0675
ERROR	1.09	4	.27		
PLACE	1.17	1	1.17	.54	.5021
Pt	.11	1	.01	.01	.9343
ERROR	8.58	4	2.17		

APPENDIX C

Table 7b. Cell Means and Standard Deviations for Kurtosis-Coronal SON

	Cell Means		
	CONTROL	LACTATING	MARGINAL
ANTERIOR	.07363	.75138	.41250
POSTERIOR	.62597	1.48301	1.03949
MARGINAL	.34980	1.10219	.72600
COUNT	3	3	6

	Standard Deviations	
	CONTROL	LACTATING
ANTERIOR	.14371	1.23376
POSTERIOR	.24802	1.81255

APPENDIX C

Statistical formulas used to compute third and fourth
moments about the mean.

By SPSS:Skew = O = Normal

< O = Platykurtic

> O = Leptokurtic

Kurtosis = O =Normal

< O = Clustered Right

> O = Clustered Left

The computing formula used by SPSS is

$$\text{Skewness} = \cfrac{\left\{\left[\sum_{i=1}^{N} X_i^3 - 3\bar{X}\left(\sum_{i=1}^{N} X_i^2\right) + 3\dot{X}^2\left(\sum_{i=1}^{N} X_i\right)\right]/N\right\} - \bar{X}^3}{\left\{\left[\left(\sum_{i=1}^{N} X_i^2\right) - N\bar{X}^2\right]/(N-1)\right\}^{3/2}}$$

the computing formula used by SPSS is

$$\text{Kurtosis} = \cfrac{\left\{\left[\sum_{i=1}^{N} X_i^4 - 4\bar{X}\left(\sum_{i=1}^{N} X_i^3\right) + 6\bar{X}^2\left(\sum_{i=1}^{N} X_i^2\right) - 4\bar{X}^3\left(\sum_{i=1}^{N} X_i\right)\right]/N\right\} + \bar{X}^4}{\left\{\left[\left(\sum_{i=1}^{N} X_i^2\right) - N\bar{X}^2\right]/(N-1)\right\}^2} - 3$$

APPENDIX C

Raw Data-Anterior Coronal SON-Control Subjects

Code	# Pixels	Mean Density
13CAA	298724.000	106.174
38CAA	203367.000	93.776
73CAA	272007.000	84.585

Code	Standard Deviation	Skewness
13CAA	31.506	-.118348
38CAA	28.858	-.351925
73CAA	29.566	.275229

Code	Kurtosis
13CAA	.195189
38CAA	.124839
73CAA	-.099146

APPENDIX C

Raw Data-Posterior Coronal SON-Control Subjects

Code	# Pixels	Mean Density
13CPA	255925.00	90.485
38CPA	271444.00	92.894
73CPA	142119.00	88.860

Code	Standard Deviation	Skewness
13CPA	25.650	.458694
38CPA	23.771	.300636
73CPA	22.780	.351697

Code	Kurtosis
13CPA	.800763
38CPA	.342105
73CPA	.735044

APPENDIX C

Raw Data—Anterior Coronal SON—Lactating Subjects

Code	# Pixels	Mean Density
91CAA	279763.000	81.118
32CAA	188891.000	87.311
51CAA	282546.000	76.886

Code	Standard Deviation	Skewness
91CAA	25.859	-.254250
32CAA	26.878	.608423
51CAA	24.563	.760567

Code	Kurtosis
91CAA	1.899755
32CAA	-.552935
51CAA	.907311

APPENDIX C

Raw Data-Posterior Coronal SON-Lactating Subjects

Code	# Pixels	Mean Density
91CPA	290002.00	84.657
32CPA	253433.00	81.762
51CPA	269900.00	81.192

Code	Standard Deviation	Skewness
91CPA	27.253	.619809
32CPA	21.977	1.325277
51CPA	24.009	.209258

Code	Kurtosis
91CPA	.684895
32CPA	3.523130
51CPA	.150995

APPENDIX C

Raw Data-Anterior Coronal LHA-Control Subjects

Code	# Pixels	Mean Density
38CAB	1353869.99	78.197
73CAB	1191411.00	69.760
13CAB	1237899.00	88.198

Code	Standard Deviation	Skewness
38CAB	24.063	.057023
73CAB	27.617	.535808
13CAB	31.828	.010854

Code	Kurtosis
38CAB	.726009
73CAB	-.008867
13CAB	.730821

APPENDIX C

Raw Data-Posterior Coronal LHA-Control Subjects

Code	# Pixels	Mean Density
38CPB	1352737.00	76.636
73CPB	1186134.00	87.772
13CPB	1198881.00	71.750

Code	Standard Deviation	Skewness
38CPB	19.156	1.177584
73CPB	21.960	.391844
13CPB	26.124	.289763

Code	Kurtosis
38CPB	2.907267
73CPB	1.989741
13CPB	.520067

APPENDIX C

Raw Data-Anterior Coronal LHA-Lactating Subjects

Code	# Pixels	Mean Density
91CAB	1362686.00	82.574
32CAB	1071292.00	91.552
51CAB	1335836.00	63.224

Code	Standard Deviation	Skewness
91CAB	21.932	.936536
32CAB	30.105	.729831
51CAB	26.490	.310911

Code	Kurtosis
91CAB	1.895950
32CAB	-.179400
51CAB	.648228

APPENDIX C

Raw Data-Posterior Coronal LHA-Lactating Subjects

Code	# Pixels	Mean Density
91CPB	1317024.00	81.235
32CPB	1369870.00	78.111
51CPB	1080481.00	74.137

Code	Standard Deviation	Skewness
91CPB	27.385	.471655
32CPB	22.621	1.326869
51CPB	24.756	.027052

Code	Kurtosis
91CPB	.564123
32CPB	2.966640
51CPB	.670475

APPENDIX C

Raw Data-Dorsal Horizontal SON-Control Subjects

Code	# Pixels	Mean Density
54HDA	367258.00	117.741
66HDA	336340.00	98.387
41HDA	298178.00	56.818

Code	Standard Deviation	Skewness
54HDA	27.611	.440625
66HDA	22.430	.406697
41HDA	19.623	.712844

Code	Kurtosis
54HDA	.405781
66HDA	.023060
41HDA	2.123982

APPENDIX C

Raw Data-Ventral Horizontal SON-Control Subjects

Code	# Pixels	Mean Density
54HVA	276707.00	120.374
66HVA	350323.00	101.216
41HVA	472037.00	71.365

Code	Standard Deviation	Skewness
54HVA	36.387	-.315331
66HAV	22.930	.366096
41HVA	23.266	.313285

Code	Kurtosis
54HVA	-.882780
66HVA	.426432
41HVA	.780499

APPENDIX C

Raw Data- Dorsal Horizontal SON-Lactating Subjects

Code	# Pixels	Mean Density
85HDA	191301.00	68.792
27HDA	340869.00	106.286

Code	Standard Deviation	Skewness
85HDA	18.747	1.031089
27HDA	33.719	.155657

Code	Kurtosis
85HDA	1.864475
27HDA	-.414626

APPENDIX C

Raw Data-Ventral Horizontal SON-Lactating Subjects

Code	# Pixels	Mean Density
85HVA	166426.00	68.145
27HVA	264407.00	99.002

Code	Standard Deviation	Skewness
85HVA	18.638	.594143
27HVA	24.039	.415365

Code	Kurtosis
85HVA	.464915
27HVA	.372381

APPENDIX C

Raw Data-Dorsal Horizontal LHA-Control Subjects

Code	# Pixels	Mean Density
54HDB	688581.00	85.556
66HDB	654511.00	84.856
41HDB	627909.00	49.468

Code	Standard Deviation	Skewness
54HDB	14.789	1.568427
66HDB	21.320	.230460
41HDB	29.673	.338521

Code	Kurtosis
54HDB	4.579433
66HDB	.412046
41HDB	-.423412

APPENDIX C

Raw Data-Ventral Horizontal LHA-Control Subjects

Code	# Pixels	Mean Density
54HVB	640015.00	81.413
66HVB	643848.00	87.382
41HVB	664010.00	67.454

Code	Standard Deviation	Skewness
54HVB	31.288	-.052896
66HVB	18.638	.594143
41HVB	21.909	.492468

Code	Kurtosis
54HVB	-.212522
66HVB	.315721
41HVB	1.568397

APPENDIX C

Raw Data-Dorsal Horizontal LHA-Lactating Subjects

Code	# Pixels	Mean Density
85HDB	522696.00	73.790
27HDB	654239.00	91.016

Code	Standard Deviation	Skewness
85HDB	21.794	.326414
27HDB	28.435	.330169

Code	Kurtosis
85HDB	.627402
27HDB	.551521

APPENDIX C

Raw Data-Ventral Horizontal LHA-Lactating Subjects

Code	# Pixels	Mean Density
85HVB	395027.00	65.900
27HVB	682863.00	71.965

Code	Standard Deviation	Skewess
85HVB	20.719	-.234204
27HVB	14.572	.936414

Code	Kurtosis
85HVB	-.008766
27HVB	3.941123